

CHAPTER 163

A MICRO-COMPUTER BASED QUASI 3-D SEDIMENT TRANSPORT MODEL

Marie-Hélène G. Briand¹ and J. William Kamphuis²

ABSTRACT

A quasi three-dimensional numerical model for detailed sediment transport calculations on a beach is developed for a micro-computer. It includes a complete description of the wave climate and wave induced currents over the study area. Vertical concentration profiles of suspended sediments, calculated locally to include the effects of shear stress on the bottom and the intensity of turbulence due to breaking waves, are superposed on local velocity profiles to yield sediment transport rates. Sediment transport is calibrated with laboratory experiments performed on a straight sand beach.

INTRODUCTION

In coastal engineering, where hydrodynamics play a major role, the latest numerical models calculating wave-induced currents and sediment transport are usually developed on large, powerful computers because of the problem's complexity. So far, detailed numerical coastal modeling has thus been largely limited to research projects. But recent innovations and rapid developments in the micro-computer industry have transformed the Personal Computer into an essential tool for scientific applications.

The present paper shows an overview of the theory used in the proposed numerical model. Briand (1990)

- ¹ Hydraulics engineer; Lalonde, Girouard, Letendre et Associés, 485 McGill street, 8th floor, Montreal, Canada, H2Y 2H4
- ² Professor, Civil Engineering, Queen's University, Kingston, Ontario, Canada, K7L 3N6

provides a detailed description of the pertinent theory and numerical methods of solution. The numerical model was developed to work efficiently on a micro-computer.

Several aspects of modeling relatively detailed coastal processes are presented with an emphasis on a simple approach to a wide range of applications. The proposed numerical model includes calculations of wave transformation, wave-induced currents and resulting sediment transport in the surf zone. Numerical results of sediment transport are calibrated with laboratory experiments. A practical "quasi" three-dimensional description of nearshore hydrodynamics and its effect on sediment transport is produced.

NUMERICAL MODEL

Wave Transformation

The model requires a discretized representation of the study area bathymetry in the form of a rectangular grid, and offshore wave conditions must be specified for either regular or random wave fields. Calculations start with a complete evaluation of the wave climate over the gridded area: shoaling, refraction, breaking and energy dissipation inside the surf zone are considered.

A Miche type of breaking criterion is used, as suggested by Goda (1970):

$$H_b = 0.17 L_o \left\{ 1 - \exp \left[-1.5 \frac{\pi d}{L_o} \left(1 + 15 m^{4/3} \right) \right] \right\} \quad (1)$$

where:

- H_b is the breaking wave height;
- L_o the deepwater wavelength;
- d the local water depth;
- m the local beach slope.

This breaking criterion was preferred to others because of its relative simplicity and because it fits better the laboratory results presented in this paper.

The principle of conservation of wave energy flux is applied to calculate wave height transformations:

$$\frac{d(Ec)}{ds} = -D \quad (2)$$

- where:
- c_g is the wave group velocity;
 - E is the total wave energy density;
 - s is the distance along the wave path;
 - D is the wave's energy dissipation rate per unit area.

It is possible to include several terms responsible for energy dissipation in Eq. 2, like friction on the bottom or percolation, but the present application considers wave breaking as the main source of dissipation. Outside the surf zone, D is equal to zero.

Energy dissipation in a breaking wave is calculated from the empirical formulation of Dally, Dean and Dalrymple (1984):

$$D = \frac{K}{d} \left[\left(E - E_{st} \right) c_g \right] \quad (3)$$

- where:
- K is an empirical coefficient;
 - E_{st} represents the "stable" energy that a breaking wave strives to attain on a constant depth bottom.

The stable energy is calculated from the stable wave height H_{st} as, suggested by Horikawa and Kuo (1966):

$$H_{st} = \Gamma d \quad (4)$$

Dally *et al* (1984) show that values of $K = 0.15$ and $\Gamma = 0.4$ give good agreement with their laboratory results.

In the wave transformation calculations, a combination of linear and cnoidal wave theories was used for a better description of wave characteristics, especially in shallow water.

In the case of a random wave field, the offshore wave spectrum is divided into several sinusoidal wave components (approximately 40 for the laboratory tests described in the second part of the present paper) with individual periods, heights, angles of approach and probabilities of occurrence. An empirical method is used to relate the components' wave heights and periods, and the probability is determined from the Rayleigh distribution of wave heights. Each regular wave component is shoaled, refracted individually and then dissipated in

the surf zone. Root-mean-square characteristics of the wave climate are calculated for comparison with measurements.

Hydrodynamics Model

For practical reasons, the complete three-dimensional (3-D) equations for hydrodynamics in the nearshore zone are not solved directly on the micro-computer. Instead, a three-step procedure is used. First, a two-dimensional representation of horizontal, time- and depth-averaged velocities and water levels (2-DH model) is developed. The horizontal velocities and local wave characteristics are then used to calculate the local vertical profiles of velocities (2-DV) at each node of the gridded area. Finally, those vertical profiles, calculated from the 2-DH current pattern, are superposed on the horizontal grid to yield what is called a "Quasi 3-D" representation of nearshore hydrodynamics.

Calculation of Velocities and Water Levels

The first step consists of calculating the time- and depth-averaged wave-induced currents \vec{u} and set-up η over the considered area. A steady state solution is obtained using an Alternate Direction Implicit formulation of the two-dimensional, horizontal (2-DH) equations of motion (Eq. 5) and continuity (Eq. 6):

$$\frac{\partial \vec{u}}{\partial t} + \left(\vec{u} \cdot \nabla \right) \vec{u} + g \nabla \eta = \frac{1}{\rho d} \left[\vec{\tau}_\ell - \vec{\tau}_b - \nabla \cdot \vec{S} \right] \quad (5)$$

$$\frac{\partial \eta}{\partial t} = - \nabla \cdot \left(\vec{u} d \right) \quad (6)$$

where the terms in Eq. 5 are respectively: the local acceleration, the non-linear convective acceleration, the hydrostatic pressure force (per unit mass), the lateral mixing shear stress, the bottom friction shear stress, and the gradient of radiation stress tensor.

To reduce instabilities and accelerate numerical computations, 2-DH calculations are performed starting with an approximation of the velocity and set-up solution based on the infinite beach simplification, i.e. variations in the longshore direction are neglected at first. Mean water depths are adjusted by the calculated wave set-up, and the coastline is allowed to shift inland to account for coastal flooding. This preliminary solution

is then introduced as the initial condition for the ADI scheme until a steady state solution is obtained. The result is a two-dimensional, horizontal current description of the study area.

Calculation of Vertical Distributions of Velocities

In the second step of the model, local vertical distributions of horizontal velocities are evaluated using an extension of Svendsen and Hansen's (1988) theoretical development for undertow, where the depth-averaged velocities calculated in step 1 are taken into account. The vertical profile of velocities is developed from a second-order differential equation for vertical momentum balance, Eq. 7, and from the principle of continuity of flow.

$$\frac{\partial}{\partial z} \left[\nu_t \frac{\partial \vec{u}}{\partial z} \right] = \frac{\partial}{\partial x_i} \left[g\eta \right] + \frac{\partial}{\partial z} \left[\vec{\nabla} \cdot \vec{S} \right] \quad (7)$$

- where:
- ν_t is the turbulent eddy viscosity;
 - x_i represents horizontal axes x and y;
 - \vec{S} is the total radiation stress tensor.

The above undertow model considers that the flow occurs in three layers. In the surface layer, between the wave crest and trough, a detailed description of the highly turbulent flow within the breaking wave roller is not necessary. The only information required is the amount of fluid carried by the roller, which is expressed in an empirical formula suggested by Svendsen (1984). A thin bottom boundary layer in which fluid viscosity is considered, includes the effect of bottom friction on the flow and accounts for steady streaming due to the wave oscillatory flow. Lastly, the middle layer flow is governed by the imbalance between the excess momentum flux induced by the breaking wave in the surface layer and the hydrostatic excess pressure created by the local mean water level gradient, or wave set-up.

Calculation of Sediment Transport

Vertical profiles of wave-induced sediment concentrations in the water column are calculated locally to be combined with vertical profiles of velocities from the hydrodynamics model to yield a quasi 3-D sediment transport pattern over the study area.

The vertical profile of sediment concentration is assumed to follow an exponential shape:

$$C(z) = C_A \exp \left(K_e \frac{(z-z_A)}{z_A} \right) \quad (8)$$

with
$$K_e = -\ln \left(C_B/C_A \right) \quad (9)$$

where: - z_A is taken as the bottom boundary layer thickness;
- C_B is the concentration at which the sediment starts moving.

The reference concentration C_A at the upper limit of the bottom boundary layer is estimated from a mobility number made up of two terms representing the individual influences of the local wave-current bottom shear stress and the turbulence created by the breaking wave:

$$C_A = \frac{K_{A1} (\nu_t/d) + K_{A2} (\tau_{wc}/\rho)^{1/2}}{w_f} \quad (10)$$

where: - K_{A1} and K_{A2} are calibration constants;
- τ_{wc} is the waves and currents shear stress;
- w_f is the sediment fall velocity.

The above sediment concentration profiles are multiplied by the local velocity profiles and integrated over the depth to yield the local sediment transport rates, in bed-load and suspended load modes. A "Quasi 3-D" description of sediment transport is obtained which is both practical and easy to solve on a micro-computer.

The above approach has a strong physical basis, and calibration of sediment transport calculations is relatively simple. Once concentration calibration parameters K_{A1} and K_{A2} , in Eq. 10, are determined, all components of sediment transport are also determined since bed-load, suspended load, longshore and cross-shore transport are coupled.

Swash Transport

The wave motion in the swash zone is a time-dependent process that is not described by the above

numerical model. However, the sediment transport contribution from the swash zone is important and must be included in some way for comparison with laboratory results. A global formulation based on the assumption that sediment concentration in the swash zone is caused only by wave energy dissipation, is proposed:

$$Q_{sw} = K_Q \left(S_{sw} \right)^{1/6} \left(L_{sh} \right)^{1/2} \frac{H_{sh}^{7/3}}{w_f} \quad (11)$$

where:

- K_Q is a calibration constant;
- S_{sw} is the swash zone width;
- L_{sh} is the wavelength at the shoreline;
- H_{sh} is the wave height at the shoreline.

Beach Morphology

Finally, each local vertical profile of sediment transport is integrated over the local water depth and included in the equation of conservation of sediment to calculate the beach morphology with time.

LABORATORY EXPERIMENTS

The numerical model was calibrated with results from experiments carried out in the wave basin of the Queen's University Coastal Engineering Laboratory. Only half of the 28 tests performed with various regular and random wave fields and two different sediment sizes were used for the present calibration (Table 1).

Wave heights, longshore currents, alongshore sediment transport rates and their cross-shore distribution were measured on a deformable sand beach. Beach profile evolution in time was monitored in detail. Wave heights and longshore currents were measured at regular intervals at many locations across the surf zone as a barred profile evolved from the initially plane beach. Sediment transport was measured using a series of 7 or 14 sand traps located at the downdrift end of the beach. Kamphuis and Kooistra (1990) provide a complete description of the laboratory set-up and test results.

To calibrate and compare the numerical model results with laboratory measurements performed on a simulated infinitely long beach, the quasi 3-D numerical model was simplified by neglecting all gradients in the alongshore direction.

Table 1. Description of laboratory tests.

Regular Test	T (sec)	H _d (cm)	D ₅₀ (mm)	Random Test	Tp (sec)	Hs _d [*] (cm)
RE	0.92	4.5	.105	IE	0.92	6.3
RF	1.15	4.5	.105	IA	1.15	4.5
RG	1.39	4.5	.105	IF	1.15	6.3
RI	1.38	6.0	.105	IG	1.39	6.3
				II	1.38	7.8
			.180	IJ*	0.92	9.0
			.180	IB	1.15	6.3
RC*	1.15	7.4	.180	IC	1.15	8.8
			.180	ID*	1.15	11.7
			.180	IK*	1.38	8.4

* Subscript "d" indicates depth at the wave generator. In all tests $d = 0.5$ m, except tests marked with a * for which $d = 0.55$ m.

RESULTS AND DISCUSSION

Numerical results for wave heights show very good agreement with measurements both inside and outside the surf zone (Fig.1), even though some regular wave experiments contained important reflection patterns.

Numerical results for longshore velocities agree well in magnitude with experiments but their cross-shore distribution does not always coincide with observations (Fig.2). This is due to the simplistic wave energy dissipation module used in the calculations. A more realistic computation should simulate the exchanges between potential, kinematic and turbulent energies, and account for the formation of a roller.

To compare longshore sediment transport rates, the swash zone contribution was separated from surf zone transport by identifying sediment traps located above mean water level. Surf zone sediment transport rates agree well with the observed results in a calibration that gives 20 times more importance to the turbulent energy dissipation term than to the bottom shear stress term in the sediment concentration calculations (Fig.3). On the other hand, swash transport predictions, based on a simple global formula that accounts only for the total wave energy dissipation on the beach face, do not agree well (Fig.4). It is of interest that the observed swash transport rates for similar wave conditions are higher for the larger sediment size (0.18 mm) than for the

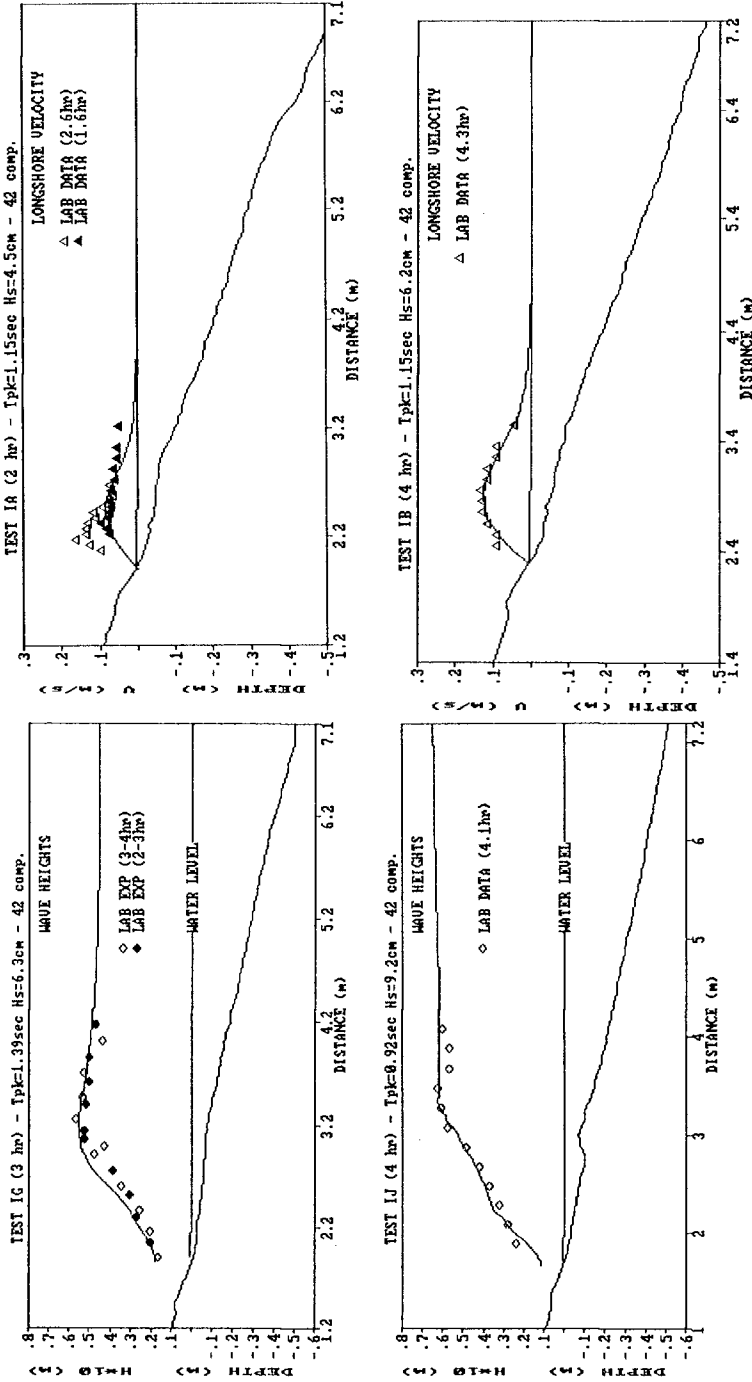


Fig. 1. Calculated and measured wave heights.

Fig. 2. Calculated and measured longshore velocities.

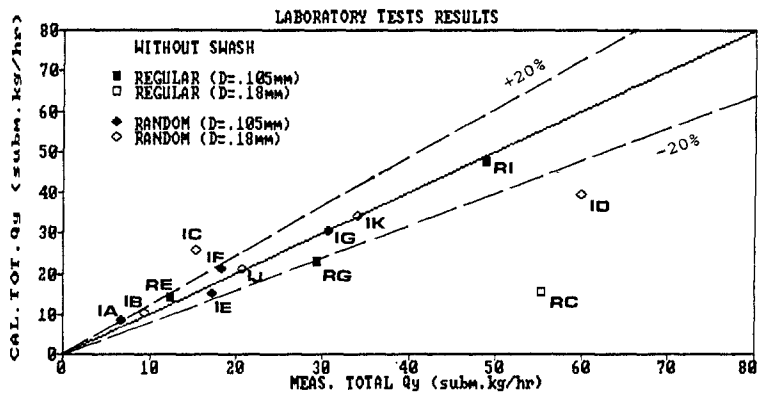


Fig. 3. Global longshore sediment transport results, without swash contribution.

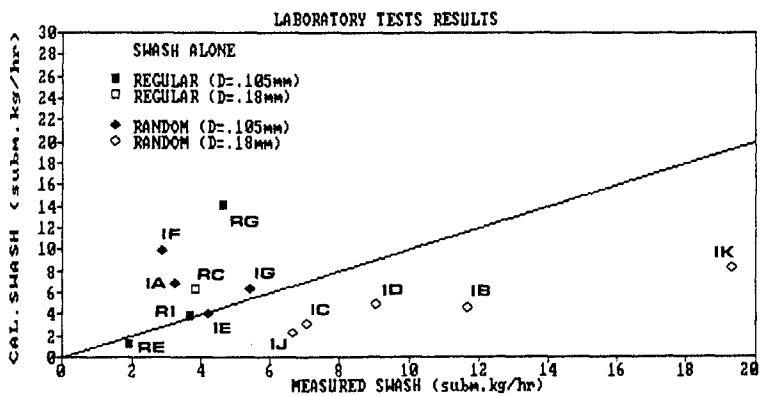


Fig. 4. Global swash transport.

smaller (0.105 mm) sand. From a comparison of calculated and measured swash transport, it is postulated that a bottom shear stress model that accounts for the critical shear stress, based on the Shields curve, would simulate the observed results better.

The calculated cross-shore distributions of long-shore sediment transport agree well with observations (Fig.5); but again, the predicted peak does not always coincide with observations. A better wave energy dissipation model should improve these results.

The numerical model is successful in predicting the proper bar location in all cases, but the observed bars are flatter than in the numerical results, indicating a lack of cross-shore convection in the undertow calculations (Fig.6). This is an effect of the quasi 3-D velocity calculations which could be improved by adding cross-shore convection artificially in the numerical scheme. The fact that swash zone processes are not taken into account in the numerical calculations can also explain the underprediction in offshore sediment transport.

Finally, Figure 7 shows a simulation of a beach profile submitted to the same wave conditions over a long period of time. After 9 hours of constant wave attack, the profile evolution slows down and the only bar transformation that still occurs is a slight accumulation of sediment on the offshore slope. The bar thus slowly moves offshore, as was observed in the laboratory.

CONCLUSIONS

The proposed quasi 3-D numerical model for sediment transport works efficiently on a micro-computer. It is also flexible, as it can account for various natural phenomena (e.g. tides, wind) by simply including additional terms in the momentum equations.

One interesting finding of the present study is that sediment transport in the surf zone is dominated by the influence of the turbulent wave energy dissipation on the sediment suspension process, whereas swash zone transport is clearly driven by the bottom shear stress effect on sediment.

There is one important limitation to the model in its present form: it should not be applied to complex bathymetries since diffraction and wave-current interactions are neglected in calculations, and because of the first approximation approach used in current calculations.

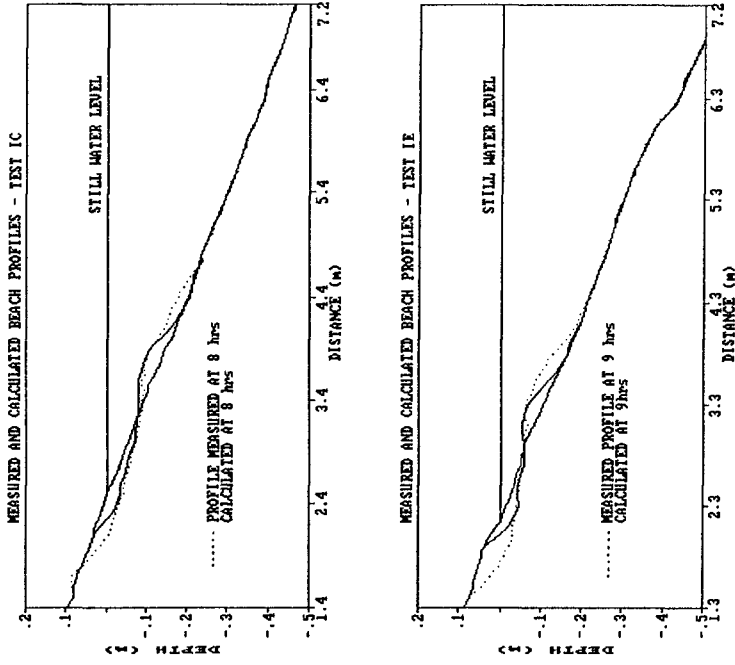


Fig. 6. Calculated and measured beach profiles.

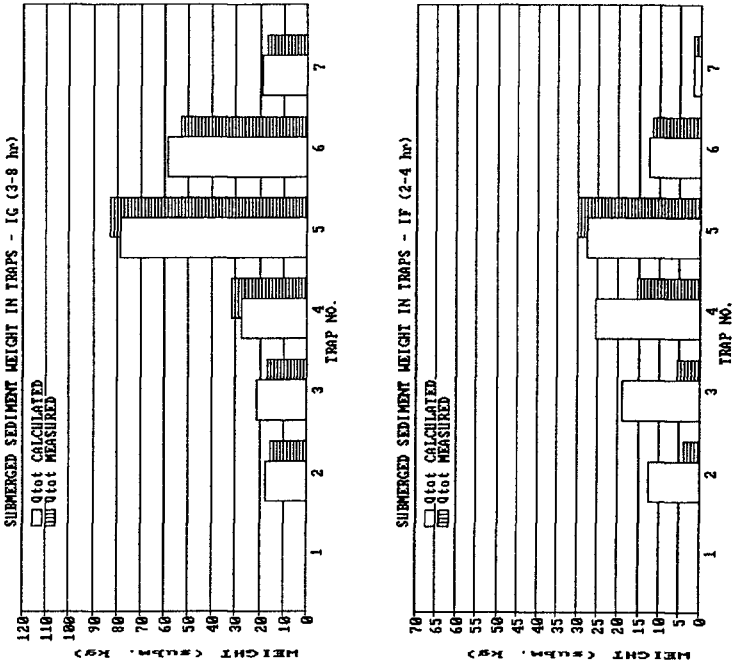


Fig. 5. Calculated and measured cross-shore distributions of longshore transport.

LONG TERM TESTING ON TEST IE - 18hrs WITH 42 COMP.

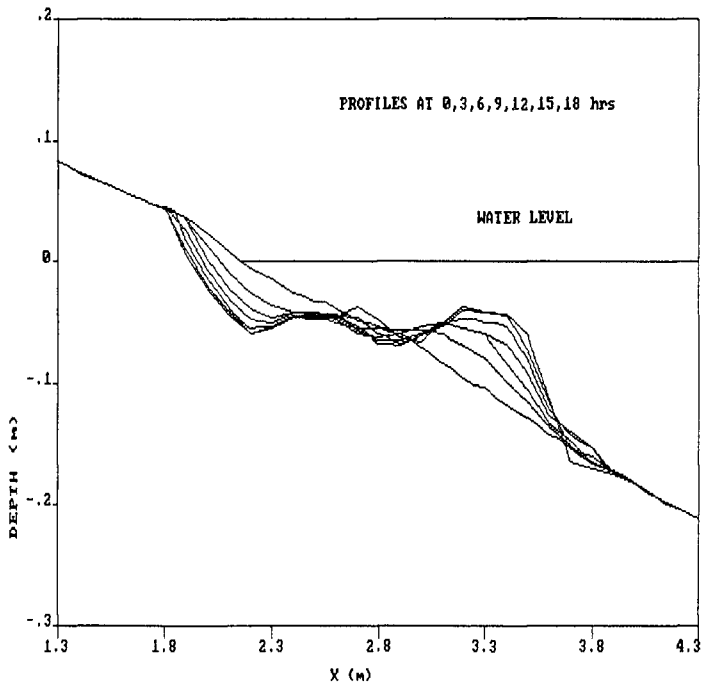


Fig. 7. Long term beach profile evolution.

Further research to improve this model will consider swash zone processes, the energy transition in breaking waves, and calibration with field measurements.

ACKNOWLEDGEMENTS

The authors gratefully recognize the financial support from the National Sciences and Engineering Research Council's Strategic and Operating Grants programs. Ms. Briand was supported from a Senator F. Carrel Award granted by Queen's University, and a Fonds F.C.A.R doctoral scholarship from the Province of Quebec. Travel grants from Queen's School of Graduate Studies and Research and the Department of Civil Engineering to present this paper are also acknowledged.

REFERENCES

- Briand, M.H.G. (1990). A detailed quasi 3-D numerical model for sediment transport processes in the surf zone. Ph.D. thesis, Queen's University, Kingston, Canada, July 1990.
- Dally, W.R., Dean, R.G., and Dalrymple, R.A. (1984). A model for breaker decay on beaches, Proc. 19th Int. Conf. Coast. Eng., ASCE, Vol.1, p.82-98.
- Goda, Y. (1970). A synthesis of breaker indices. Trans. of Japan Soc. of Civ. Eng., Vol.2, No.2, p.227-230.
- Horikawa, K. and Kuo, C.T (1966). A study on wave transformation inside the surf zone. Proc. 10th Int. Conf. Coast. Eng., ASCE, p.217-233.
- Kamphuis, J.W. and Kooistra, J. (1990). Three dimensional mobile bed hydraulic model studies of wave breaking, circulation and sediment transport processes. Proc. of the Canadian Coastal Conference, Kingston, Canada, May 1990, p.363-386.
- Svendsen, I.A., and Hansen, J.B. (1988). Cross-shore currents in surf zone modelling. Coast. Eng., 12, p.23-42.
- Svendsen, I.A. (1984). Mass flux and undertow in a surf zone. Coastal Eng., 8, p.347-365.